X-ray Studies on the Structure of Polyacrylonitrile Fibers

X. D. Liu and W. Ruland*

Department of Physical Chemistry and Center for Materials Science, University of Marburg, Hans-Meerwein-Strasse H, W-3550 Marburg/Lahn, Germany

Received November 11, 1992

ABSTRACT: Using an X-ray fiber diffractometer, 2D intensity distributions of homopolymer polyacrylonitrile (PAN) fibers are measured in reciprocal space in the plane containing the fiber axis. The equatorial intensity distributions show four relatively sharp reflections and three diffuse maxima. The sharp reflections correspond to a pseudohexagonal 2D lattice of intermolecular packing. The diffuse maxima are due to the Laue scattering of a rotational disorder in this lattice. The off-equatorial intensity distribution is mainly determined by intramolecular scattering. A comparison with calculated 2D intensity distributions for various conformations of short PAN chain segments reveals that the predominant conformation is planar zigzag. 2D correlation functions obtained by Fourier transformation of the intensity distribution corroborate this interpretation. To reconcile the results of the WAXS studies with tacticity measurements using ^{13}C NMR, the continuity of the zigzag conformation is considered to be interrupted by defects (kinks) related to sterically unfavorable sequences of CN groups. No evidence is found for the existence of a two-phase structure with ordered and disordered domains.

1. Introduction

Polyacrylonitrile (PAN) fibers are widely used as textile and reinforcement fibers as well as precursors for carbon fibers. There have been a number of structural studies on PAN fibers,[1-10] but a clear picture of the intramolecular and intermolecular structure is still missing. Since technical PAN is an atactic polymer, molecular conformation and packing is expected to be imperfect. The normal beam WAXS fiber pattern of a well-oriented PAN fiber shows on the equator a rather strong and relatively sharp reflection with a Bragg spacing $d \simeq 5.2$ Å, a diffuse maximum with $d \simeq 3.3$ Å, and a weak but relatively sharp reflection with $d \simeq 3$ Å. All off-equatorial reflections are diffuse. The diffuse equatorial maximum with $d \simeq 3.3$ Å is interpreted by various authors[11-13] as an "amorphous halo", and its intensity relative to the sharp reflections is used to determine an amorphous content. The concept of ordered and disordered domains existing in PAN fibers seems to be supported by the temporary appearance of a meridional maximum in the SAXS during heat treatment of PAN fibers in the range of 200–300 °C.[14-18] This meridional SAXS maximum is, however, absent in the pristine fiber.

The aim of the present work is to use improved methods of WAXS measurement and evaluation to obtain more detailed information on the fiber structure. In the Theoretical Section, specific problems encountered in the evaluation of disordered fiber structures are treated. The results of this treatment are used together with information obtained from molecular modeling to evaluate the experimental data.

2. Theoretical Section

For the evaluation of the experimental data we use a simplified model for the structure and the packing of the PAN chains. In analogy to the WAXS of polycrystalline materials, we consider the WAXS to be the sum of the contributions of representative structural units (RSU). In the RSU, the chains are considered to be oriented with their principal axes parallel to the main axis of the RSU. The packing is taken to be pseudohexagonal; i.e., the distances between the chain axes form an imperfect 2D hexagonal lattice in which the chains are rotated randomly about their axis. Finally, the average contribution of a RSU to the total WAXS is represented by the cylindrical average of its intensity distribution in reciprocal space about its principal axis. Finite preferred orientation can be produced by defining the intensity distribution of a RSU in polar coordinates and introducing axial orientation distributions of finite width with the help of integral transforms or developments into series of Legendre polynomials.[19]

The average RSU contains N chains of length L_3. The latter parameter is considered to be a coherence length of the chain conformation within the RSU and is, in general, much smaller than the total length of a chain. The intensity I_U of a RSU is given by

$$I_U = N(\langle\langle|F_M|^2\rangle_N\rangle_\psi - |\langle\langle F_M\rangle_N\rangle_\psi|^2 D) + |\langle\langle F_M\rangle_N\rangle_\psi|^2 D\langle|Z_P|^2\rangle_\psi \quad (1)$$

where F_M is the structure factor of a chain, $\langle\ \rangle_N$ is the average over all chains in a RSU, $\langle\ \rangle_\psi$ is the average over all orientations about the main axis of a chain or of the RSU, D is a general disorder function taking into account the effect of thermal motion and displacement disorder on the interchain distances, and Z_P is the 2D lattice factor of the pseudohexagonal packing of the chains. Equation 1 represents a special case of substitutional disorder.

The importance to consider the average over N separate from the average over ψ is seen in the case where we consider the backbone of a PAN chain to remain in the planar zigzag conformation within a length L_3 while the orientation of the CN groups is statistical (see Figure 1a). The average scattering intensity of such a chain is given by

$$\langle\langle|F_M|^2\rangle_N\rangle_\psi = n(\langle\langle|F_0|^2\rangle_n\rangle_\psi - \langle|\langle F_0\rangle_n|^2\rangle_\psi)C + \langle|\langle F_0\rangle_n|^2\rangle_\psi|Z_M|^2 \quad (2)$$

where n is the number of monomers per chain, $\langle\ \rangle_n$ the average over all monomers, F_0 the structure factor of a monomer, C the correlation function of the CN group positions, and Z_M the 1D lattice factor of the sequence of monomers along the chain. Furthermore

$$|\langle\langle F_M\rangle_N\rangle_\psi|^2 = |\langle\langle F_0\rangle_n\rangle_\psi|^2|Z_M|^2 \quad (3)$$

* To whom correspondence should be addressed.

0024-9297/93/2226-3030$04.00/0

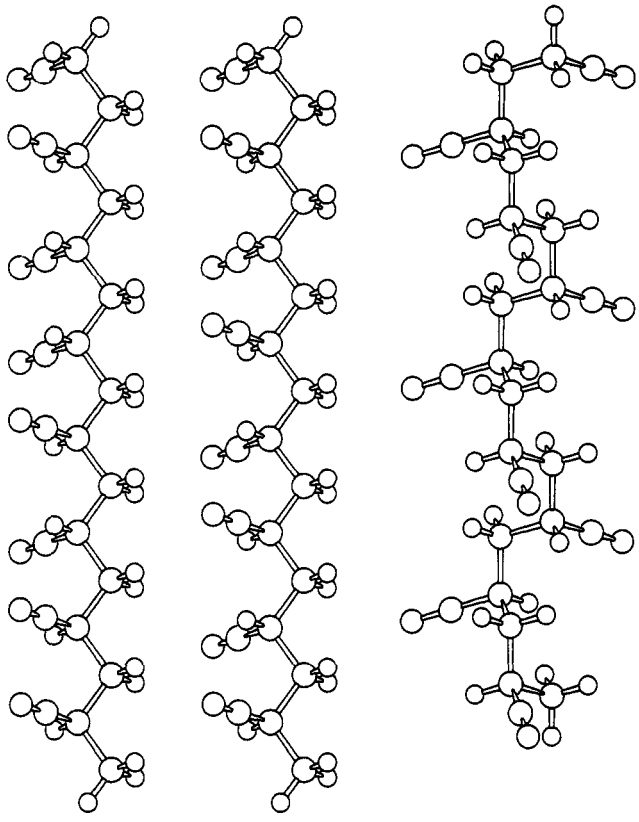

Figure 1. Molecular models for the chain conformation in PAN: (a) atactic with planar zigzag, (b) syndiotactic, (c) isotactic.

Inserting eqs 2 and 3 into eq 1, we obtain

$$I_U = Nn(\langle\langle|F_0|^2\rangle_n\rangle_\psi - \langle|\langle F_0\rangle_n|^2\rangle_\psi)C + N(\langle|\langle F_0\rangle_n|^2\rangle_\psi - |\langle\langle F_0\rangle_n\rangle_\psi|^2 D)|Z_M|^2 + |\langle\langle F_0\rangle_n\rangle_\psi|^2 D\langle|Z_P|^2\rangle_\psi|Z_M|^2$$

If the chains in the pseudohexagonal packing are shifted randomly with respect to each other parallel to the main axis, the intermolecular interferences are concentrated on the equator; i.e., the intensity distribution I_{eq} in the vicinity of the equator is given by

$$I_{eq} = [N(\langle|\langle F_0\rangle_n|^2\rangle_\psi - |\langle\langle F_0\rangle_n\rangle_\psi|^2 D) + |\langle\langle F_0\rangle_n\rangle_\psi|^2 D\langle|Z_P|^2\rangle_\psi]|Z_{M0}|^2 \quad (4)$$

where $|Z_{M0}|^2$ is the region of $|Z_M|^2$ in the vicinity of the equator. The off-equatorial intensity distribution is then determined by the intramolecular scattering $N\langle\langle|F_M|^2\rangle_N\rangle_\psi$ alone.

If is of interest to note that the first term on the right-hand side of eq 4 is nonzero only if the average over n does not include the average over ψ, i.e., if the statistical sequence of the orientation of the CN groups along the chain does not produce a random twist of the backbone.

The explicit forms of the functions used for the calculation are as follows:

$$\langle\langle F_0|^2\rangle_n\rangle_\psi = c_1\langle|F_{01}|^2\rangle_\psi + c_2\langle|F_{02}|^2\rangle_\psi$$

$$\langle|\langle F_0\rangle_n|^2\rangle_\psi = \langle|c_1F_{01} + c_2F_{02}|^2\rangle_\psi$$

$$|\langle\langle F_0\rangle_n\rangle_\psi|^2 = |c_1\langle F_{01}\rangle_\psi + c_2\langle F_{02}\rangle_\psi|^2 = |\langle F_{01}\rangle_\psi|^2 = |\langle F_{02}\rangle_\psi|^2$$

$$\langle|\langle F_0\rangle_n|^2\rangle_\psi - |\langle\langle F_0\rangle_n\rangle_\psi|^2 = c_1c_2\langle|F_{01} - F_{02}|^2\rangle_\psi$$

where c_i is the concentration of the CN group orientation i (1 or 2) and F_{0i} is the structure factor of the monomer of type i. Considering Markov chain statistics of first order,[20,21] we obtain for infinitely long chains

$$C = \frac{1 - p^2}{1 + p^2 - 2p\cos 2\pi a_3 s_3}$$

with

$$p = p_{11} + p_{22} - 1$$

where p_{ij} is the probability that the CN group orientation i is followed by the orientation j (Markov chain of first order). If $p = 0$, then there is no correlation (Bernoullian statistics); if $-1 < p < 0$, then alternating sequences are preferred; if $0 < p < 1$, then sequences of equal orientation are preferred. a_3 is the repeat distance of the backbone structure, and s_3 the component of the reciprocal space vector $\mathbf{s} = (s_1, s_2, s_3)$ in the direction of the principal axis in an orthogonal system of coordinates ($s = |\mathbf{s}| = 2\sin(\theta/\lambda)$), $s_{12} = (s_1^2 + s_2^2)^{1/2}$

$$\langle|F|^2\rangle_\phi = \sum_{j=1}^{m}\sum_{k=1}^{m} f_j f_k J_0(2\pi r_{jk} s_{12})\cos(2\pi z_{jk} s_3)$$

$$\langle F\rangle_\phi = \sum_{j=1}^{m} f_j J_0(2\pi r_j s_{12})\exp(2\pi i z_j s_3)$$

where m is the number of atoms in the monomer unit, f_i is the atomic scattering factor of atom j, J_0 is the Bessel function of the first kind of order 0, and (x_j, y_j, z_j) are the coordinates of the atom j.

$$r_{jk} = [(x_j - x_k)^2 + (y_j - y_k)^2]^{1/2}$$

$$r_j = [(x_j - x_0)^2 + (y_j - y_0)^2]^{1/2}$$

where (x_0, y_0) are the coordinates of the axis of rotation for the average over ϕ.

$$|Z_M|^2 = n\frac{1 - H^2}{1 + H^2 - 2H\cos(2\pi a_3 s_3)}$$

$$H = \exp[-(2\pi^2\sigma_3^2 s_3^2 + 2a_3/L_3)]$$

where σ_3 is the variance of a_3. Accordingly

$$|Z_{M0}|^2 = n\frac{L_3}{a_3(1 + \pi^2 L_3^2 s_3^2)}$$

In order to take into account the finite length of the chains and the variance of a_3 in C, we replace the statistics parameter p by $p_{eff} = pH$.

$$D = \exp(-ks_{12}^2)$$

where $k = 4\pi^2\langle u^2\rangle$ and u is the displacement of the chain axis from its ideal position in the 2D lattice.

$$\langle|Z_P|^2\rangle_\psi = \frac{N}{2\pi A_0}\sum_{h\geq 1}\sum_{0\leq k\leq h}\frac{m_{hk}}{s_{hk}} I_{hk}(s_{12} - s_{hk})$$

where $A_0 = a_1^2 3^{1/2}/2$ is the surface of the 2D unit cell, a_1 is the average distance between the chain axes, (hk) is the index of the 2D reciprocal lattice, m_{hk} is the multiplicity ($m_{00} = 1$, $m_{h0} = m_{hh} = 6$, $m_{hk} = 12$), $s_{hk} = 2(h^2 + k^2 + hk)^{1/2}/(a_1\sqrt{3})$ is the absolute value of the reciprocal space vector $\mathbf{s}_{hk}$, and I_{hk} are normalized line profiles with the integral width B_{hk}.

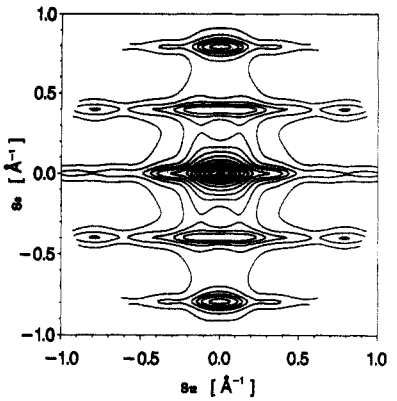

Figure 2. Calculated intramolecular scattering for an atactic chain of PAN with a planar zigzag conformation and Bernoullian statistics with $c_1 = c_2 = 0.5$ and $L_3 = 10$ Å.

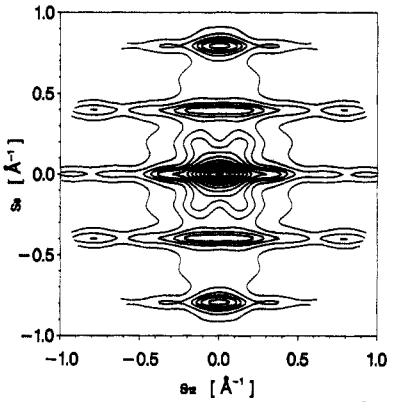

Figure 3. Calculated intramolecular scattering for an atactic chain of PAN with a planar zigzag conformation and first-order Markov chain statistics with $c_1 = c_2 = 0.5$, $p = -0.5$, and $L_3 = 10$ Å.

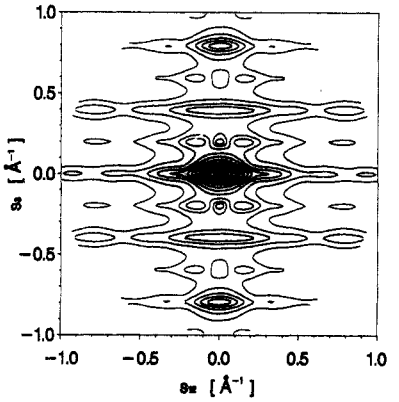

Figure 4. Calculated intramolecular scattering for a syndiotactic chain of PAN with a planar zigzag conformation.

Figures 2–5 show a comparison of calculated intramolecular intensity distributions (isointensity contour plots) in the plane (s_{12}, s_3) corresponding to the range in s accessible to a fiber diffractometer using Cu radiation. Figures 2–4 correspond to PAN chains with a planar zigzag conformation of the backbone, $c_1 = c_2 = 0.5$ and $p = 0$, −0.5, and −1, respectively. Figure 5 corresponds to an isotactic PAN chain with a 3/1 helix conformation (see Figure 1c). The diagrams show that a clear distinction is possible between the planar zigzag and the 3/1 helix as well as between Bernoullian statistics ($p = 0$) and Markov statistics ($p < 0$) in the case of a planar zigzag. For the calculations, the parameters L_3 and σ_3 were taken to be 10 Å and 0, respectively.

Figure 6 shows the intensity along the equator corresponding to chain structures with a planar zigzag con-

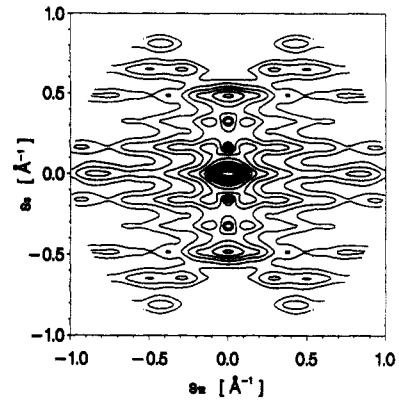

Figure 5. Calculated intramolecular scattering for an isotactic chain of PAN with a 3/1 helix conformation.

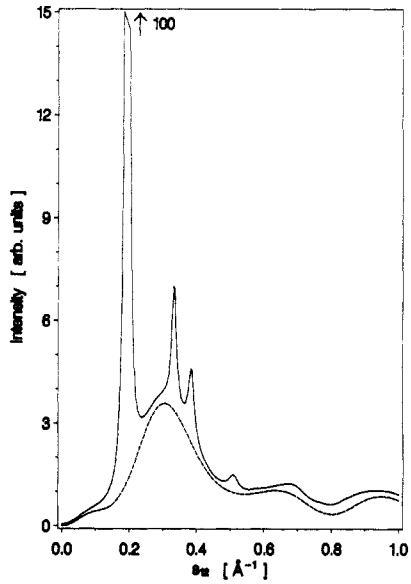

Figure 6. Calculated equatorial scattering for a pseudohexagonal packing of PAN chains with a planar zigzag conformation and rotational disorder. Solid line: total intensity. Dotted line: diffuse disorder scattering produced by the term $\langle|\langle F_0\rangle_n|^2\rangle_\psi - |\langle\langle F_0\rangle_n\rangle_\psi|^2$ in eq 4.

formation of the backbone and $c_1 = c_2 = 0.5$. Since the intensity distribution on the equator is determined by the projection of the RSU onto a plane perpendicular to the principal axis, there is no difference between a strictly alternating sequence and a statistical one as long as the planar zigzag conformation is preserved. The parameters used for the calculation are $a_1 = 6.00$ Å, $B_{hk} = (0.004 + 0.2\ s_{hk}^2)$ Å^{-1}, $k = 0$, and Cauchy-type line profiles. The summation over hk was such that $0 < s_{hk} \leq 1.3$ Å^{-1} to ensure that the contribution of the tails of higher order maxima was properly taken into account. The axis of rotation of the chains was considered to be defined by the centers of the carbon atoms in the backbone to which the CN groups are linked. A variation of the position of the axis of rotation leads to changes in the shape and position of the first diffuse maximum. Inspection of Figure 6 reveals that the intensity distribution on the equator is composed of sharp and diffuse maxima. The former, produced by the lattice factor $|Z_P|^2$, decrease strongly in intensity due to the structure factor $|\langle\langle F_0\rangle_n\rangle_\psi|^2$ even if $D = 1$. The latter, produced by the term $|\langle F_0\rangle_n|^2\rangle_\psi - |\langle\langle F_0\rangle_n\rangle_\psi|^2$, show a rather intense maximum at $s_{12} \simeq 0.3$ Å^{-1} and two maxima of lower intensity at $s_{12} \simeq 0.66$ and 0.93 Å^{-1}. This demonstrates that the diffuse equatorial maximum with a Bragg spacing of about 3.3 Å is not a proof for the existence of a two-phase system of ordered and disordered domains.

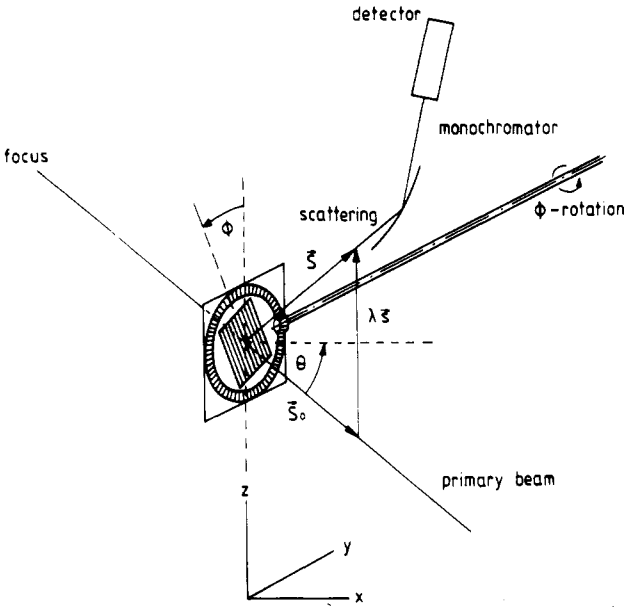

Figure 7. Schematical representation of the scattering geometry.

3. Experimental Section

The PAN fibers investigated in the present study are technical PAN homopolymer fibers (<0.7% methyl acrylate) produced by Hoechst (Dolanit). As-spun ("unrelaxed") fibers have initial tensile moduli E of about 17–20 GPa, tensile strengths σ_B of about 0.8–1 GPa, and extensions at break ϵ_B of about 8–10%. Fibers treated in hot steam ("relaxed") show a reduced initial tensile modulus (about 7–10 GPa) and tensile strength (about 0.5–0.7 GPa) but increased extension at break (about 15–17%). Samples of an unrelaxed and a highly relaxed fiber were chosen for the WAXS studies.

Using ^{13}C NMR for determining the tacticity of the fibers, the triad frequencies 27% mm, 50% mr, and 23% rr were obtained. This corresponds to a Bernoullian statistics with a small preference for the m diad; i.e., the fibers have a randomly atactic structure.

X-ray studies of preferred orientation and order–disorder phenomena in fibers require precise measurements of scattering intensities over large regions in reciprocal space. Due to the cylindrical symmetry of the samples, only a planar section in reciprocal space containing the cylinder axis needs to be investigated. For the present studies, the scattering geometry shown in Figure 7 has been chosen which is similar to an experimental setup described in an earlier paper.[22] $\mathbf{S}_0$ and $\mathbf{S}$ are unit vectors defining the direction of the primary and the scattered beam, respectively. By definition, the difference between $\mathbf{S}$ and $\mathbf{S}_0$ is $\lambda\mathbf{s}$, where λ is the X-ray wavelength. In order to increase the intensity yield and to simplify absorption corrections, a great number of fibers are mounted parallel on a frame with a homogeneous coverage. The frame is fixed on a sample holder in such a way that the plane formed by the parallel fibers is perpendicular to the plane defined by $\mathbf{S}$ and $\mathbf{S}_0$ and parallel to $\mathbf{s}$. The latter condition is maintained by the usual $\theta/2\theta$ ratio between the movements of the sample holder and the counter. The frame can be rotated within the plane formed by the parallel fibers; the angle of rotation is ϕ. The rotation is transmitted by conical gears to an axis through the center of the diffractometer and can be set by hand or by a synchronous motor. Varying θ and keeping ϕ fixed, measurements are made along straight lines passing through the origin of reciprocal space. For fixed θ and varying ϕ the measurements follow concentric circles in reciprocal space with the radius s. This setting is used for the determination of orientation distriutions and for measurements of the spherical average of the intensity distribution of a fiber. In the latter case, the intensity $I(s,\phi)$ is multiplied with $|\sin\phi|$ before summing the data for a complete cycle in ϕ.[23] For measurements of undistorted 2D intensity distributions in reciprocal space, a special computer program was used which calculates θ and ϕ values corresponding to a rectangular raster in $s_{12} = s\sin\phi$ and $s_3 = s\cos\phi$, controls the angular settings by synchronous motors, and collects the intensity data. Further treatment of the data includes correction for absorption, polarization, and Compton scattering.

A curved monochromator between the sample and counter is used to reduce the divergence of the scattering and to attenuate the Compton scattering.

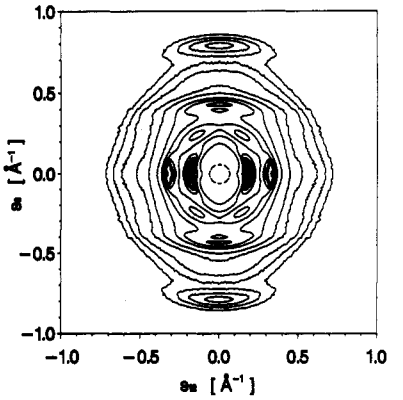

Figure 8. 2D intensity distribution for an unrelaxed PAN fiber.

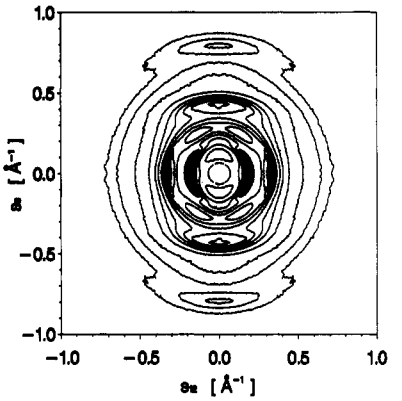

Figure 9. 2D intensity distribution for a relaxed PAN fiber.

4. Results and Discussion

4.1. 2D Intensity Distributions. Figures 8 and 9 show experimental 2D intensity distributions (isointensity contour plots) of an unrelaxed and a relaxed PAN fiber, respectively, corrected for polarization and absorption. These plots have been computed from intensity data measured on a square raster of (s_{12}, s_3) values with $\Delta s = 0.01$ Å^{-1}. A qualitative comparison of the experimental intensity distributions outside of the equator with Figures 2–5 exhibits a strong similarity with the patterns given in Figures 3 and 4, corresponding to the intramolecular scattering of a PAN chain with planar zigzag conformation and a preference for syndiotactic sequences. No resemblance appears to exist between the experimental patterns and that of Figure 5 (3/1 helix of isotactic sequences; see Figure 1), whereas Figure 2 shows similarities in the intensity distribution near the meridian. The meridional maximum at $s_3 \simeq 0.8$ Å^{-1} of the experimental intensity distributions corresponds to a repeat distance a_3 of 2.525 (unrelaxed) and 2.509 Å (relaxed) in the projection of the structure onto the fiber axis. This is in accordance with a planar zigzag conformation as the predominant conformation of the chains. From the width of this meridional maximum, a coherence length of $L_3 \simeq 14$ Å is obtained for both types of fibers. If the diffuse off-meridional maximum with the approximate coordinates $s_{12} = 0.2$ Å^{-1} and $s_3 = 0.2$ Å^{-1} is considered to be an intramolecular interference, the distribution of the CN group orientation along the chain should have a preference for syndiotactic sequences (r diads). This is in contradiction to the results of the ^{13}C NMR which show clearly a Bernoullian statistics

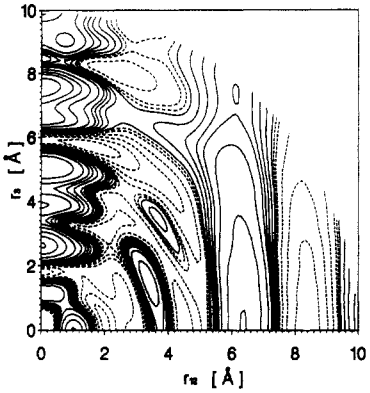

Figure 10. 2D atomic correlation function for an unrelaxed PAN fiber.

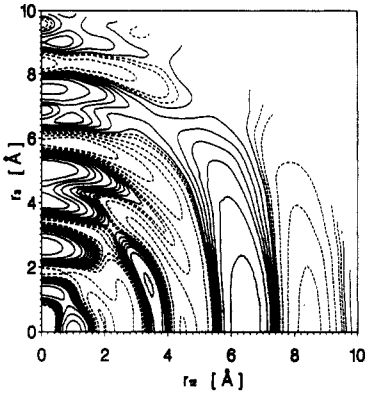

Figure 11. 2D atomic correlation function for a relaxed PAN fiber.

of the m and r diads. On the other hand, if the diffuse off-meridional maximum is supposed to be an intermolecular interference, there should be a preferred positional correlation between adjacent chains parallel to the chain axes with a periodicity of about two monomer units. Such a periodicity in the positional correlation implies a corresponding periodicity in the structure of the chains which is again in contradiction with the NMR results.

4.2. Fourier Transformation of the 2D Intensity Distributions. Since the 2D intensity distributions have been measured with reasonable accuracy, a Fourier transformation of the data to obtain the 2D atomic correlation function $P(r_{12},r_3)$ of the structure[24] is expected to produce further information on the molecular conformation and the packing. Due to the cylindrical symmetry of the intensity distribution in reciprocal space, this transformation is given by

$$P(r_{12},r_3) = 2\pi \int_{s_{12}} \int_{s_3} s_{12} I_{at}(s_{12},s_3)\, J_0(2\pi r_{12} s_{12}) \times \cos(2\pi r_3 s_3)\, ds_{12}\, ds_3 + \langle \rho_{at} \rangle_v \quad (5)$$

where

$$I_{at} = \frac{I - I_{inc}}{N_{at}\langle f^2 \rangle} - 1$$

I_{inc} is the incoherent (Compton) scattering, N_{at} is the number of atoms in the irradiated volume of the sample, and $\langle f^2 \rangle$ is the number average of the square of the atomic scattering factor.

$$\langle \rho_{at} \rangle_v = \langle \rho \rangle_v (\bar{Z}/Z^2) \quad (6)$$

where $\langle \rho \rangle_v$ is the average electron density and Z the number of electrons per atom. For the computation of I_{inc}, the attenuation of the Compton scattering due to the monochromator has to be taken into account.[25] Due to the monochromatization of the scattered radiation, the Compton scattering was nearly completely suppressed at higher values of s.

Contour plots of $P(r_{12},r_3) - \langle \rho_{at} \rangle_v$ are shown in Figures 10 and 11 corresponding to the unrelaxed and the relaxed PAN fibers, respectively. Solid lines correspond to positive values and dotted lines to negative values. Cut-off ripples have been effectively suppressed by multiplying I_{at} with a smoothing function of the type $\exp(-as^n)$ with $a = 0.9$ and $n = 10$. Since s_{max} is 1.0 Å^{-1}, the resolution of details in the correlation function is approximately 0.8 Å due to the cut-off error. This means that a number of intramolecular distances are at least partially superposed. Furthermore, it has to be taken into account that the correlation functions of the experimental data are affected by the orientation distribution of the chain axes with respect to the fiber axis which results in a supplementary broadening in ϕ. From the orientation distributions of the main equatorial reflections we obtain widths of about 14° for the unrelaxed and about 28° for the relaxed fiber. The following features are observable:

1. In the vicinity of the fiber axis, a series of maxima is visible which can be associated with the C–C distances of the backbone of the planar zigzag conformation. Using the positions of seven peaks for a linear fitting, we obtain an average value of $a_3 = 2.573$ Å for the unrelaxed and $a_3 = 2.530$ Å for the relaxed fiber.
2. In the direction perpendicular to the fiber axis, there are two peaks which can be related to partially superposed C–H, C–C, and C–N distances perpendicular to the chain axis as expected for the planar zigzag conformation.
3. The maxima with the coordinates $r_{12} \simeq 3.4$ Å and $r_3 \simeq 1.4$ Å visible for both types of fibers and the maximum at $r_{12} \simeq 3.7$ Å and $r_3 \simeq 3.5$ Å visible only for the unrelaxed fiber can be correlated to distances between the carbon atom of the CH_2 group and the nitrogen atom of the same and of the adjacent monomer unit, respectively.
4. For both types of fibers, there are broad distributions of intermolecular distances at $r_{12} \simeq 6.4$ Å extending parallel to the fiber axis. These distributions do not show any significant modulations in the direction of the fiber axis. The streak connecting these distributions to maxima in the vicinity of the fiber axis appears to be produced by the orientation distribution of the chain axes.

Thus, the results of the Fourier transformation confirm the interpretation of the intensity distributions concerning the most probable conformation of the chain structure. In addition, they give further evidence for a random translation of adjacent chains parallel to the chain axes, i.e., no specific positional correlations between atoms located in different chains except the parallelism of the chain axes.

4.3. Equatorial Intensity Distributions. The intensity distribution on the equator for the unrelaxed fiber is shown in Figure 12 in a semilog plot of $s_{12}I(s_{12},0)$. The multiplication with s_{12} compensates the decrease of the intensity due to the finite preferred orientation. For the relaxed fiber, a very similar curve is obtained. In both cases, four relatively sharp reflections and three diffuse maxima are observed. The positions of the sharp reflections correspond to the indices (10), (11), (20), and (21) of a 2D hexagonal lattice with the lattice constant $a_1 = 6.044$ Å for the unrelaxed and 6.039 Å for the relaxed fiber. No evidence for the existence of an orthorhombic lattice[2,4,7,8,10] (e.g., splitting of reflections) can be observed. A semiquantitative evaluation of the widths of the reflections as functions of the position leads to a lattice size parameter of about 180 Å for the unrelaxed and 100 Å for the relaxed fiber. The positions of the diffuse maxima

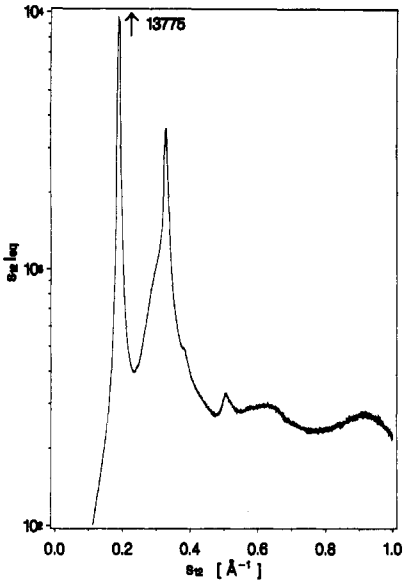

Figure 12. Equatorial intensity distribution of an unrelaxed PAN fiber.

are at s_{12} = 0.30, 0.61, and 0.95 Å^{-1} in both cases. A comparison of Figure 12 with Figure 6 shows clearly the strong resemblance between the theoretically predicted and the experimentally observed curves. Furthermore, the orientation distribution of the diffuse maximum at 0.30 Å^{-1} was found to be essentially the same as that of the (10) and the (11) reflections. Thus, the interpretation of the diffuse maximum at s_{12} = 0.30 Å^{-1} as being due to the rotational disorder in the packing of the chains appears to be justified. No evidence for a two-phase system of ordered and disordered domains has been detected. In any case, an interpretation of the maximum at s_{12} = 0.30 Å^{-1} in terms of an amorphous halo would imply that the intermolecular distances in the disordered domains are about 37% shorter than those in the ordered domains, which is highly unlikely.

4.4. Molecular Modeling. If we consider the basic structure of PAN fibers to consist of a homogeneously disordered pseudohexagonal packing of chains with a planar zigzag cnformation, two problems have to be solved. First, the theoretical density for such a fiber structure calculated on the basis of the unit cell dimensions obtained from the X-ray diffraction data is 1.10 g/cm^3, whereas the experimental value of the density is 1.17–1.22 g/cm^3. Second, we have to explain why the 2D intensity distributions contain interference maxima which can be related to Markov statistics of the orientation of the CN groups with a preference for syndiotactic sequences, whereas the results of the ^{13}C NMR show definitely that PAN is atactic with a Bernoullian statistics of the r and m sequences.

Both problems can be solved if we assume that the planar zigzag conformation is discontinuous; i.e., it is interrupted at irregular intervals by kinks. Models for such kinks are given in Figure 13. We assume that short isotactic sequence can be accommodated in the planar zigzag conformation in spite of the unfavorable dipole interaction between adjacent CN groups. However, the stability of the planar zigzag conformation will be very low for longer isotactic sequences. On the other hand, the 3/1 helix conformation requires rather long isotactic sequences to become stable and it cannot accommodate syndiotactic sequences. The energy of interaction in isotactic sequences with a planar zigzag conformation can be effectively reduced by kink formation. A kink of the type tg^+tg^-t does not change the general orientation of the chain but

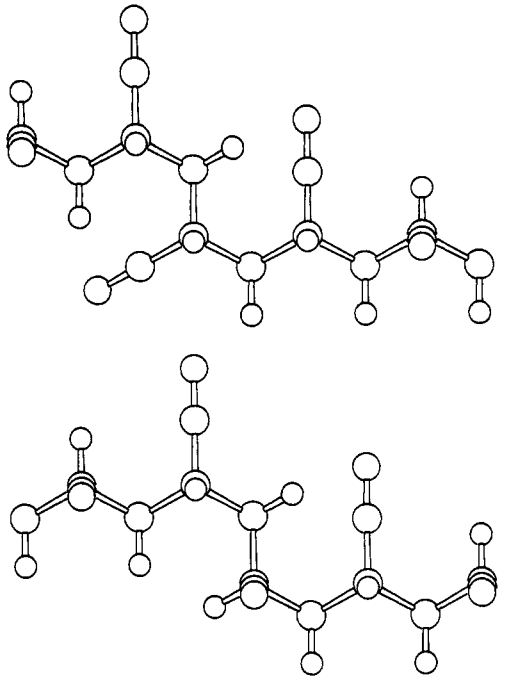

Figure 13. Zigzag chain of PAN with kinks at isotactic sequences.

leads to an increase of the number of monomer units per chain length in the projection onto the chain axis. A simple calculation shows that the difference between the theoretical and the experimental value of the density could be explained by about 1 kink per 10 monomer units. In this case, the average coherence length of the planar zigzag conformation would correspond roughly to the L_3 value of 14 Å derived from the 2D intensity distributions. Since the kink formation eliminates isotactic sequences, the remaining chain sections with zigzag conformation contain more syndiotactic sequences than predicted by the Bernoullian statistics. This would explain the existence of interference maxima related to an enhanced occurrence of syndiotactic sequences observed in the 2D intensity distributions.

Due to their low concentration and statistical distribution, a direct observation of kink structures in X-ray scattering cannot be expected. Molecular modeling of a densely packed ensemble of atactic PAN chains would be desirable for the investigation of the conformation of the chains under the influence of intramolecular and intermolecular interactions. However, the complexity of such calculations exceeds, at least at present, our computational possibilities. To obtain information on the intramolecular interaction alone, we have carried out dynamic molecular modeling calculations using the program SYBYL on a single atactic PAN chain containing 50 monomer units. Starting from a planar zigzag conformation, various semistable conformations can be obtained by increasing the thermal mobility. If the temperature is too high, we obtain random-coil conformations.

At moderate temperatures, chain conformations as shown in Figure 14 are observed. If we assume that a kink is formed under the influence of intermolecular interactions in the parallel stacking of chains at those positions where there is a change of the direction of the backbone in the single chain, we obtain approximately the expected concentration of kinks discussed above.

4.5. Kinks and Mechanical Properties. The concept of kinks has a consequence for the mechanical properties of PAN fibers. If the chain conformation would be a continuous planar zigzag (as predicted for syndiotactic PAN) and the preferred orientation would be sufficiently

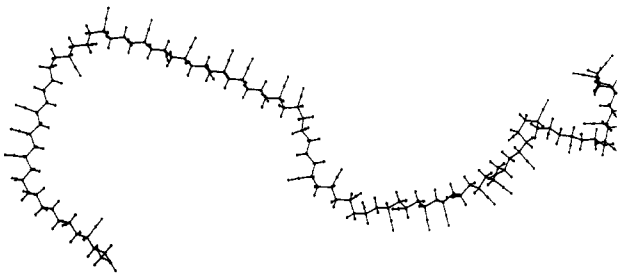

Figure 14. Molecular modeling of a single atactic PAN chain with moderate thermal mobility.

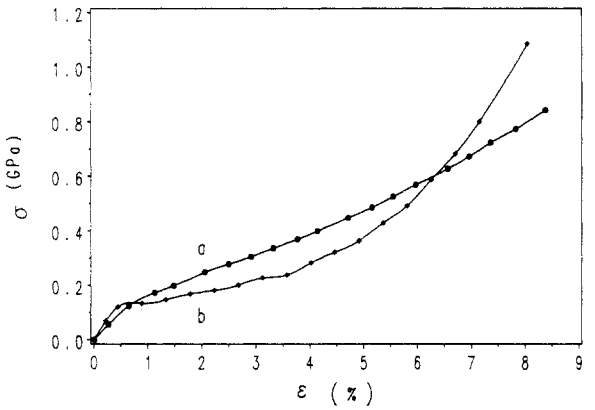

Figure 15. (a) Theoretical and (b) experimental stress–strain curves for an unrelaxed PAN fiber.

high, the fibers would have initial tensile moduli comparable to those of ultrahigh modulus polyethylene or poly(*p*-phenyleneterephthalamide). The measured tensile moduli are, however, about 1 order of magnitude lower. In order to investigate the possible influence of kinks on the stress–strain behavior of PAN fibers, the deformation of single chains with kinks has been calculated using an MM3 program. The change of the energy as a function of the increase of the end-to-end distance of an atactic chain consisting of 10 monomer units and 1 kink was used, together with the number of chains per cross section derived from X-ray data, to calculate a theoretical stress–strain curve.

Although the approximations used in this calculation are rather crude, the result shows a strong resemblance to the experimental stress–strain curve for the unrelaxed PAN fiber as can be seen in Figure 15. The initial tensile modulus is found to be about $^1/_4$ of that of an ideal syndiotactic chain. The intermediate decrease and final increase of the modulus with increasing strain is due to a torsion of the kink. The steep increase of the stress at about 8% strain corresponds to the elimination of the kink and is very close to the experimental value of the extension at break of the unrelaxed fiber.

If kinks have an influence on the mechanical properties in the way discussed here, a decrease of the kink concentration would result in a substantial increase of the initial tensile modulus. The synthesis of pure syndiotactic PAN has so far not been successful. However, any method of synthesis which increases statistically the amount of syndiotactic sequences would presumably lead to a decrease of the formation of kinks and, consequently, to an increase of the initial modulus and the tensile strength but also to a decrease of the extension at break.

5. Conclusions

The results of the present study can be summarized as follows:

1. The conformation of the PAN chains is predominantly planar zigzag with a finite persistence along the chain.

2. The finite persistence can be explained by kinks related to the occurrence of isotactic sequences. The concept of kinks is in accordance with the density and, at least qualitatively, with the stress–strain behavior of the fibers.

3. The packing of the chains is pseudohexagonal. No positional correlations except the parallel arrangement exist between adjacent chains.

4. The rotational disorder about the chain axes produces a diffuse scattering maximum in the equatorial scattering. This maximum has been interpreted hitherto as an "amorphous" halo and used for the evaluation of the "crystallinity" of PAN. No evidence for the existence of a two-phase system was found in our studies.

The theoretical treatment of the rotational disorder in the parallel packing of rodlike chains and the appearance of diffuse scattering maxima together with sharp reflections should be of general interest for the evaluation of the scattering of rigid-rod polymer structures.

Acknowledgments. The authors are indebted to the Deutsche Forschungsgemeinschaft for support of this work. The provision of the PAN fiber samples by Hoechst AG is gratefully acknowledged. Thanks are also due to Mr. C. Burger for assistance in computation and helpful discussions.

References and Notes

(1) Houtz, R. C. *Text. Res. J.* **1950**, *20*, 786.
(2) Stéfani, R.; Chevreton, M.; Garnier, M.; Eyraud, C. *C. R. Hebd. Seances Acad. Sci.* **1960**, *251*, 2174.
(3) Bohn, C. R.; Schaefgen, J. R.; Statton, W. O. *J. Polym. Sci.* **1961**, *55*, 531.
(4) Holland, V. F.; Mitchell, S. B.; Hunter, W. L.; Lindenmeyer, P. H. *J. Polym. Sci.* **1962**, *62*, 145.
(5) Lindenmeyer, P. H.; Hosemann, R. *J. Appl. Phys.* **1963**, *34*, 42.
(6) Klement, J. J.; Geil, P. H. *J. Polym. Sci., Polym. Phys. Ed.* **1968**, *6*, 1381.
(7) Hinrichsen, G.; Orth, H. *J. Polym. Sci., Polym. Lett. Ed.* **1971**, *9*, 529.
(8) Colvin, B. G.; Storr, P. *Eur. Polym. J.* **1974**, *10*, 337.
(9) Gupta, A. K.; Chand, N. *Eur. Polym. J.* **1979**, *15*, 899.
(10) Kumamaru, F.; Kajiyama, T.; Takayanagi, M. *J. Cryst. Growth* **1980**, *48*, 202.
(11) Hinrichsen, G. *J. Polym. Sci.* **1972**, *C38*, 303.
(12) Gupta, A. K.; Chand, N. *Eur. Polym. J.* **1979**, *15*, 899.
(13) Gupta, A. K.; Singhal, R. P. *J. Polym. Sci., Polym. Phys. Ed.* **1983**, *21*, 2243.
(14) Tyson, C. N. *Nature, Phys. Sci.* **1971**, *229*, 121.
(15) Fillery, M. E.; Goodhew, P. J. *Nature, Phys. Sci.* **1971**, *233*, 118.
(16) Hinrichsen, G. *J. Appl. Polym. Sci.* **1973**, *17*, 3305.
(17) Warner, S. B. *J. Polym. Sci.: Polym. Lett.* **1978**, *16*, 287.
(18) Warner, S. B.; Uhlmann, D. R.; Peebles, L. H. *J. Mater. Sci.* **1979**, *14*, 1893.
(19) Ruland, W. *Colloid Polym. Sci.* **1977**, *255*, 833.
(20) Bonart, R.; Mulzer, G.; Dietrich, J. *Makromol. Chem.* **1987**, *188*, 637.
(21) Bonart, R. *Makromol. Chem.* **1987**, *188*, 1187.
(22) Ruland, W. *Norelco Rep.* **1967**, *14*, 12.
(23) Ruland, W.; DeWaelheyns, A. *J. Sci. Instrum.* **1967**, *44*, 236.
(24) Vineyard, G. H. *Acta Crystallogr.* **1951**, *4*, 281.
(25) Ruland, W. *Br. J. Appl. Phys.* **1964**, *15*, 1301.